MICROEARTHQUAKE MOMENT TENSORS FROM THE COSO GEOTHERMAL AREA

Bruce R. Julian,
U. S. Geological Survey
345 Middlefield Rd., MS977
Menlo Park, CA, 94025, USA
e-mail: julian@usgs.gov

G. R. Foulger,
Dept. of Earth Sciences, Durham University
Durham, DH1 3LE, UK
e-mail: g.r.foulger@durham.ac.uk

Francis Monastero
Geothermal Program Office , US Navy
1 Administration Circle
China Lake, CA, 93555-6001, USA
e-mail: francis.monastero@navy.mil

ABSTRACT

The Coso geothermal area, California, has produced hot water and steam for electricity generation for more than 20 years, during which time there has been a substantial amount of microearthquake activity in the area. Seismicity is monitored by a high-quality permanent network of 16 three-component digital borehole seismometers operated by the US Navy and supplemented by a ~ 14-station portable array of surface three-component digital instruments. The portable stations improve focal sphere coverage, providing seismic-wave polarity and amplitude data sets sufficient for determining full moment-tensor microearthquake mechanisms by the linear-programming inversion method. We have developed a GUI-based interface to this inversion software that greatly increases its ease of use and makes feasible analyzing larger numbers of earthquakes than previously was practical.

We show examples from an injection experiment conducted in well 34-9RD2, on the East Flank of the Coso geothermal area. This tight well was re-drilled February – March 2005 with the intention of hydrofracturing it, but instead, pervasive porosity and fractures were encountered at about 2660 m depth. Total drilling mud losses occurred, obviating the need to stimulate the well. These mud losses induced a 50-minute swarm of 44 microearthquakes, with magnitudes in the range -0.3 to 2.6. Most of the largest microearthquakes occurred in the first 2 minutes. Accurate relative relocations and moment tensors for the best-recorded subset reveal fine details of the fracture that was stimulated. This comprised a fault striking at N 20° E and dipping at 75° to the WNW, which propagated to the NNE and upward. Co-injection focal mechanisms reveal combined crack-opening and shear motion. Stress release and mode of failure differed between the pre-, co- and post-swarm periods. Some post-swarm events involved cavity collapse, suggesting that some of the cavity opening caused by the fluid injection was quickly reversed. Stress & mode of failure had not returned to pre-swarm conditions within 1 month following the injection, posing the question of how long stress perturbations persist following a stimulation experiment. This question may be answered by processing data spanning a longer post-injection period, work that is currently underway and will be reported in this presentation.

INTRODUCTION

The full moment-tensor source mechanisms of microearthquakes at geothermal areas provide information, particularly about seismic volume changes, that conventional "fault-plane solutions" do not and that are potentially valuable for understanding physical processes accompanying activities such as energy extraction and fluid injection. Moment tensors for microearthquakes at several geothermal areas in Iceland (Miller *et al.*, 1998), California (Ross *et al.,* 1999), and Indonesia (Foulger, proprietary results) show significant seismic volume increases and decreases that are

correlated with industrial activities such as injection and production.

Interpretation of moment tensors in terms of physical processes, however, is non-unique; different processes can produce identical seismic wave fields, and thus identical moment tensors (Julian *et al.*, 1998). To overcome this limitation, moment tensors must be supplemented by other kinds of information to narrow the range of possible interpretations. Recently developed methods for determining the relative locations of earthquakes with high resolution (*e.g.* Waldhauser and Ellsworth, 2000), which delineate the geometry of seismic failure regions, are valuable in this respect. Foulger *et al.* (2004) recently used this combination of methods to show that many naturally occurring microearthquakes at Long Valley caldera, California, are caused by tensile failure.

This paper describes ongoing studies applying the same techniques to the Coso geothermal area, in the southwestern Basin Range province in California. We show results for microearthquakes that occurred during a brief but intense swarm on 3 March 2005 when drilling at well 39-9RD2 encountered a permeable zone a sudden a sudden loss of drilling mud occurred, and also microearthquakes before and after this swarm.

METHOD

Most methods for determining moment tensors are applicable only to earthquakes larger than about magnitude 4, and earthquakes this large are rare in geothermal areas. To overcome this limitation, we invert seismic wave first-motion polarities jointly with amplitude ratios, using linear programming methods (Julian, 1986; Julian and Foulger, 1996). Amplitude ratios are greatly preferable to raw amplitudes for this purpose because they can be chosen to be relatively immune to distortion by wave-propagation effects such as geometric spreading by three-dimensional heterogeneity in the Earth. We used this method in all of the moment-tensor studies referenced above.

RESULTS

Figure 1 shows moment-tensor mechanisms for eight microearthquakes from the 3 March 2005 swarm. They are all similar in having volume increases, and could be explained by faulting on NNE-striking planes dipping either WNW or ESE, combined with some other process involving approximately isotropic volume increases.

The high-resolution hypocenter locations shown on the right-hand side of Figure 2, however, rule out such interpretations. They clearly resolve a NNE-striking fault, but it dips steeply, with an orientation between those of the hypothetical normal faults, and

passes through the middle of the dilatational *P*-phase polarity fields, as shown on the top left plot of Figure 1. This orientation is just that expected for a tensile fault consistent with the derived moment tensors.

The volume changes indicated by the moment tensors, however, are smaller than those for pure tensile faults, as Figure 3 shows. The "source types" shown on this kind of plot depend only on the ratio of the principal moment, and are independent of both source strength (scalar moment) and source orientation. Pure tensile faults lie at the "+Crack" point on such plots, and combinations of tensile and shear faulting lie near, and to the right of, the line connecting the +Crack point with the center of the plot. The observed moment tensors, in contrast, lie below and to the left of this line, and indicate some volume-compensating process such as flow of fluid into the opening crack.

Figure 3 also shows source types for microearthquakes before and after the swarm, and Figure 4 shows source orientations for these three sets of events. The swarm-event source types closely correspond to those expected for tensile faulting, with an additional partial volume-compensation, as discussed above. Significant numbers of events during the other two time periods lie in the right half of the source-type plot, indicating geometrically complex shears, and, after the swarm, in the lower half of the plot, indicating volume decrease.

CONCLUSIONS

Full moment-tensor source mechanisms, which can be determined accurately for geothermal microearthquakes by jointly inverting seismic wave polarities and amplitude ratios, provide valuable information about volume changes accompanying geothermal processes. Their physical interpretation is non-unique, however, and requires extra information such as that provided by recently developed methods of locating microearthquake hypocenters with high relative resolution.

Application of these methods at the Coso geothermal area shows that a swarm of microearthquakes accompanying rapid fluid loss at well 39-9RD2 in March 2005 was caused by tensile faulting, probably accompanied by rapid fluid flow into the opening crack. A further EGS experiment at Coso will be studied later this year, with a view to extending our understanding the physical processes at work.
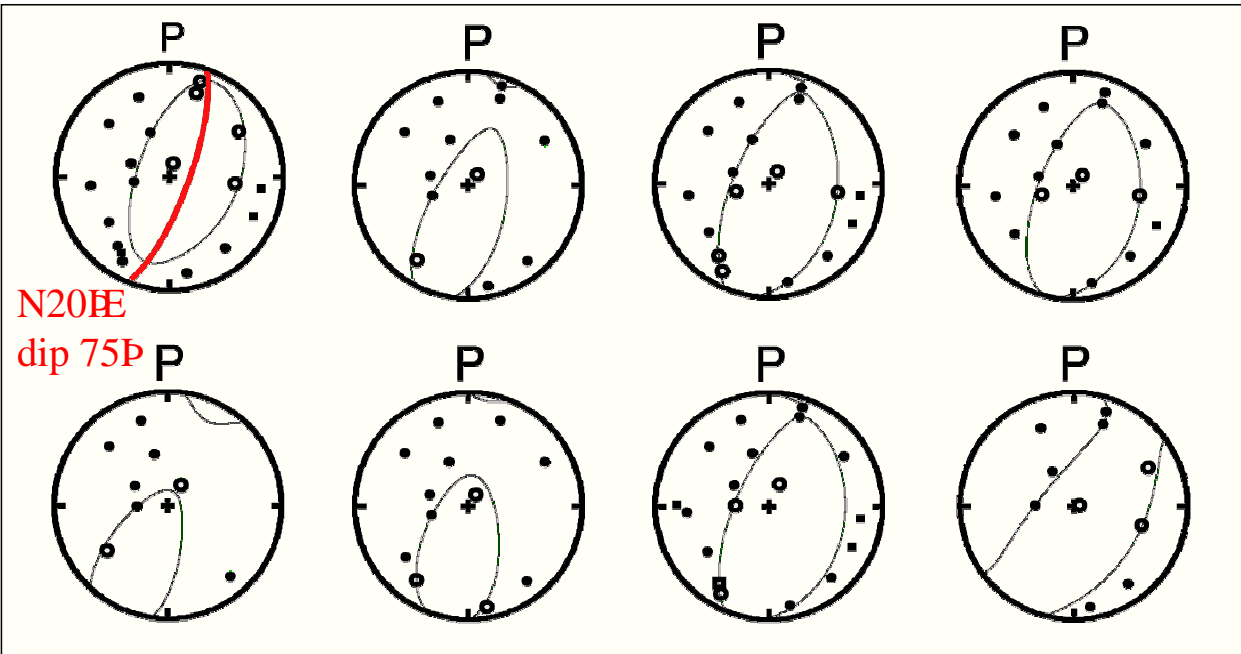
N20ÞE
dip 75Þ

Figure 1.   Upper hemisphere focal sphere plots for co-swarm earthquakes. Black dots indicate compressional first P-wave arrivals and open circles indicate dilatational arrivals. The mechanisms are very uniform and resemble normal-faulting mechanisms, but with reduced dilatational fields, indicating net explosive (i.e., cavity opening) components in the source. The fault plane defined by the accurately relatively relocated earthquakes is plotted as a red line on the top left focal sphere, and bisects the dilatational field.
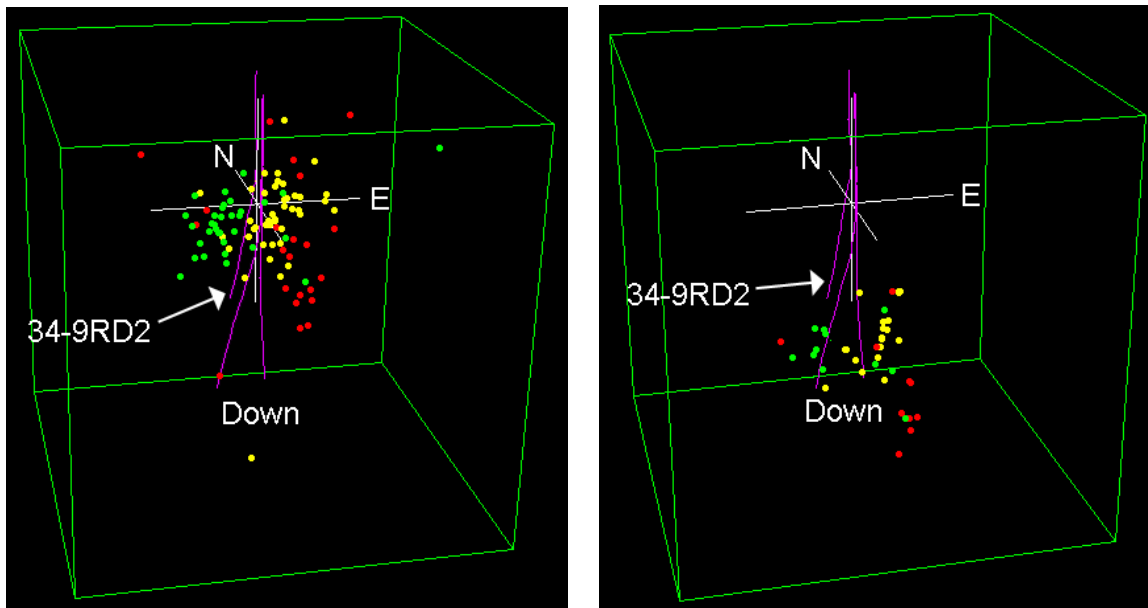

Figure 2.   Three-dimensional perspective views of (green) pre-, (yellow) co- and (red) post-swarm earthquake locations, along with (magenta) the trajectories of boreholes. Left: US Navy catalog locations, right: relatively relocated locations. The catalog locations comprise a diffuse cloud that reveals little information of use concerning details of the seismically active fracture network. In contrast, the co-swarm relative relocations clearly delineate a N 20° E-trending plane leading from the bottom of the borehole cluster. Furthermore, the relatively relocated earthquake population is located deeper, near the base of the boreholes, a more likely scenario than the much shallower locations obtained from the catalog.
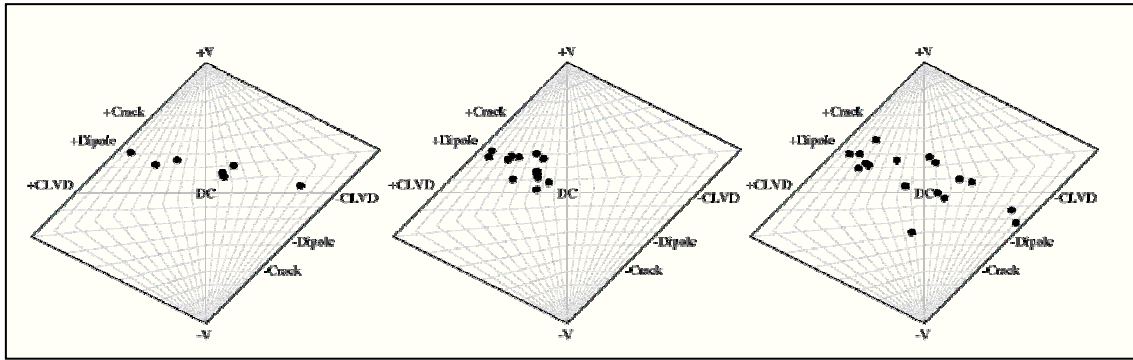
Figure 3.   Source-type plots showing (left) pre-, (middle) co- and (right) post-swarm earthquakes. The three groups clearly comprise different populations, reflecting different seismic fracture styles during the three periods. Prior to the swarm, the mechanisms had small or positive volume changes, indicating shear faulting and cavity opening. During the swarm, the volume change component tended to be larger. No co-swarm events had negative "CLVD" components (i.e., no events plot in the right-hand side of the diagram). This contrasts with the pre-swarm earthquakes, but its significance is not clear. The post-swarm earthquakes included additionally earthquakes with cavity closing source components (i.e., plotting in the lower half of the figure) suggesting that the crack that opened during the fluid injection had already started to close in the weeks immediately following.
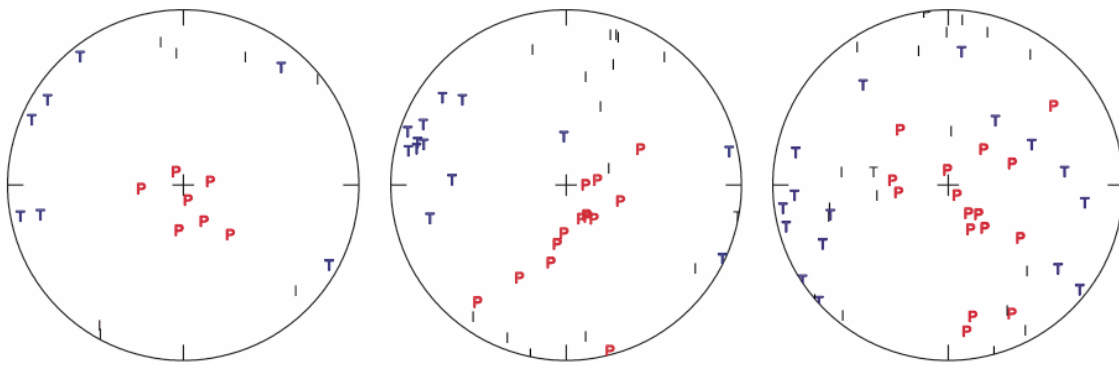

Figure 4.   Pressure (P, red), Tension (T, blue) and Intermediate (I, black) axes for the (left) pre-, (middle) co- and (right) post-swarm earthquakes. These roughly correspond to the greatest, least and intermediate principal stresses σ_1, σ_3 and σ_2. The three groups clearly indicate seismic stress release in response to different stress conditions.

REFERENCES

Foulger, G.R., Julian, B.R., Hill, D.P., Pitt, A.M., Malin, P.E., and Shalev, E. (2004), "Non-double-couple microearthquakes at Long Valley caldera, California, provide evidence for hydraulic fracturing", *J. Volcanol. Geotherm. Res.*, **132**, 45-71.

Julian, B.R. (1986), "Analysing seismic-source mechanisms by linear-programming methods", *Geophys. J. R. Astr. Soc.*, **84**, 431-443.

Julian, B.R., Miller, A.D., and Foulger, G.R. (1998), "Non-double-couple earthquakes I. Theory", *Rev. Geophys.*, **36**, 525-549.

Julian, B.R., and Foulger, G.R. (1996), "Earthquake mechanisms from linear-programming inversion of seismic-wave amplitude ratios", *Bull. Seismol. Soc. Am.*, **86**, 972-980.

Miller, A.D., Julian, B.R., and Foulger, G.R. (1998), "Three-dimensional seismic structure and moment tensors of non-double-couple earthquakes at the Hengill-Grensdalur volcanic complex, Iceland", *Geophys. J. Int.*, **133**, 309-325.

Ross, A., Foulger, G.R., and Julian, B.R. (1999), "Source processes of industrially-induced earthquakes at The Geysers geothermal area, California", *Geophysics*, **64**, 1877-1889.

Waldhauser, F., and Ellsworth, W.L. (2000), "A double-difference earthquake location algorithm: Method and application to the northern Hayward fault, California", *Bull. Seismol. Soc. Am.*, **90**, 1353-1368.